Morphological changes on annealing polyethylene single crystals

Stephen J. Spells
Division of Applied Physics, Sheffield City Polytechnic, Pond Street, Sheffield S1 1WB, UK

and Mary J. Hill
H. H. Wills Physics Laboratory, University of Bristol, Tyndall Avenue, Bristol BS8 1TL, UK
(Received 27 April 1990; revised 19 September 1990; accepted 19 September 1990)

The annealing of polyethylene single crystals has been studied using time-dependent X-ray diffraction. The behaviour of the small-angle diffraction peak is found to depend on both the temperature of annealing (T_a) and on the rate of heating to that temperature. For a heating rate of 10°C min^{-1} and $T_a \leqslant 123$°C, the results are consistent with a localized solid state reorganization. Using a heating rate of 500°C min^{-1} for any T_a or using a heating rate of 10°C min^{-1} for $T_a > 123$°C resulted in a dramatic loss of peak intensities at intermediate times, consistent with larger scale melting. Transmission electron micrographs of annealed samples show an improvement in lamellar orientation for heating at 500°C min^{-1} and $T_a > 120$°C. Small angle X-ray data give no indication of this improvement. To reconcile these results, we propose a domain structure for the annealed samples and present supporting evidence from electron microscopy for domain boundaries.

(Keywords: morphology; annealing; polyethylene)

INTRODUCTION

The irreversible thickening of lamellar crystals during heating has been found to be a general feature of polymer behaviour. Polyethylene has been most widely studied in this respect, with numerous reports of increasing long period with annealing time on the evidence of small-angle X-ray scattering (SAXS) measurements[1,2]. A logarithmic increase in long period with annealing time has been observed[1], although more recent measurements using either a synchrotron source[3] or a high intensity conventional source[4] have enabled earlier stages of annealing to be observed. These show an initial induction period, followed by a rapid increase in long period, with a third region characterized by a logarithmic increase in long period with time.

The influence of heating rate on morphological changes within polymers during annealing is well established: the variation in position of the melting endotherm in polyethylene has been reported as a function of heating rate for various starting morphologies. Differential scanning calorimetry (d.s.c.) measurements may show two melting endotherms, one resulting from material which has reorganized during heating and another from material which has not, with the peak positions and relative intensities dependent on heating rate.

It has long been held that mechanisms of localized solid state diffusion and partial melting/recrystallization may occur under different conditions (of temperature, heating rate, etc.). As part of a wider programme of study on the annealing process in polyethylene single crystals, we have made time-dependent SAXS measurements at two different heating rates. These are reported here, with the aim of identifying any indication of differences in annealing mechanisms in the two cases: the results are correlated with structural information obtained from the final materials using electron microscopy.

ANNEALING PROCESS

Most previous work on annealing has involved the use of relatively low heating rates (around 10°C min^{-1}) to attain the annealing temperature. Under these conditions, it is convenient to consider annealing in three temperature regimes[6]. In the first, there is no change in long period, although other structural changes occur. The intermediate regime has been the focus of recent studies of molecular mobility[6,7]; it has been concluded from combined neutron scattering and infra-red spectroscopy that a localized solid state thickening process occurs. In these recent studies, it was found useful to discuss annealing processes in terms of a length scale (L_a) over which the sample is simultaneously molten at a particular annealing temperature. In this intermediate temperature region, the conformational models required to give agreement with both infra-red and neutron scattering data indicated that $L_a \ll R_g$ (where R_g is the radius of gyration). The distance scale of regions with enhanced molecular mobility was therefore sufficiently small for the process to be termed a 'solid state transformation', since truly molten regions of any significant size are not present. Nevertheless, the real extent of molecular mobility is still a matter of conjecture. Evidence, for example, of isolated chain segments with sufficient mobility to be considered as completely molten is not available and so this question is not pursued in the present work. In the third temperature region (highest

0032-3861/91/152716-08

temperatures) there is, by contrast, clear evidence of partial melting. One aim of the present work is to determine whether the heating rate affects the transition from the second to the third annealing regime. In addition, we suspected that the final morphologies, if achieved by different processes, might appear different when viewed in the transmission electron microscope.

The availability of intense X-ray beams from synchrotron radiation has allowed the study of lamellar organization at an early stage of annealing. Studies of solution crystallized polyethylene have been made at both high[3,8] heating rates and, using a high intensity conventional source, at low[4,9] heating rates. With two exceptions[4,8] these measurements were made on unfractionated polymer. Grubb *et al.*[3], using heating rates as high as 1300°C min^{-1}, showed that annealing was a three-stage process. An initial induction period characterized by a small increase in long period was followed by a very rapid increase in spacing (although these two stages were not observed for $T_a > 125$°C). In the final stage, the well known logarithmic time dependence of the long period was observed. An initial decrease in the scattered intensity was interpreted as evidence of melting prior to recrystallization. This view was supported by later parallel wide-angle X-ray scattering (WAXS) and SAXS measurements[8]. A sample of narrow molecular weight fraction showed annealing at longer times progressing with a constant long period, in contrast to the logarithmic behaviour of unfractionated material.

Measurements at lower heating rates (up to 10°C min^{-1}) using a high intensity rotating anode source and proportional counter[4] involved a large spacing between data points. This necessitated a curve-fitting procedure to obtain intensities and spacings. The results showed similar behaviour to those of Grubb *et al.*[3] although unusual behaviour was observed for higher annealing temperatures; following an initial rapid rise in long period, a decrease to a constant plateau level was observed, before the predicted eventual slow increase in long period. The resulting peak in the long period was an unexpected feature; we suggest that it is a consequence of the broad molecular weight distribution for the sample. This gives rise to a distribution of crystal thicknesses, with thinner crystals melting first on heating. However, the plateau in the long period at intermediate annealing times was generally observed. Analysis of these data using a Monte Carlo simulation based on a rate equation model[9] led to the conclusion that both partial and local melting were involved at higher values of T_a and only partial melting at lower T_a.

The X-ray work described above demonstrates the need for measurements to be made on similar samples at different heating rates, in order to establish whether heating rate is important in determining the mechanism of annealing. Furthermore, the reversible increases in long period noted above show the necessity of using samples of narrow molecular weight fractions with well-defined starting morphologies. The work presented here involves time-dependent X-ray measurements made during annealing, using different heating rates. In addition, annealed samples have been examined in the electron microscope, to establish any morphological differences arising from changes in either heating rate or T_a.

Quantitative X-ray analysis

In recent SAXS work, considerable use has been made of the scattering invariant, Q, defined as the total scattering power for an experiment using pinhole collimation:

$$Q = \int_0^\infty I(s)s^2 \, ds \tag{1}$$

where $I(s)$ is the scattered intensity at wavevector s ($s = 2 \sin \theta/\lambda$, 2θ = scattering angle, λ = X-ray wavelength). For a simple two phase system, Q is related to the overall crystallinity (X_c) and the difference in electron density between crystalline and amorphous phases:

$$Q = KX_c(1 - X_c)(\rho_c - \rho_a)^2 \tag{2}$$

The constant K includes geometrical factors for the instrument used and ρ_c and ρ_a are the electron densities for crystalline and amorphous phases respectively.

During an annealing experiment, changes in Q may therefore arise either from changes in crystallinity or through changes in density of the different phases. Additionally, the two-phase approximation, upon which equation (2) is based, may become increasingly valid during the course of annealing as the fold surface becomes more regular. Schouterden *et al.*[10] used empirical relationships for the physical densities of crystalline and amorphous phases in low- and high-density polyethylene[11] to calculate changes in X_c during heating of melt crystallized samples. However, such a method does not take account of the influence of morphology on the density of phases: the application of density data for one sample morphology to samples with different structure, types of defect and fold surface can be of very limited validity.

For these reasons, we consider the use of the invariant to be unjustified in the present case. The evolution of X_c during annealing is best studied using WAXS measurements. Unfortunately, simultaneous small- and wide-angle measurements at the synchrotron radiation source (SRS) (SERC Daresbury Laboratory, UK) are currently not feasible.

Sample preparation

The sample used was prepared from Rigidex 50 by liquid–liquid fractionation. Molecular weight, $\bar{M}_w$, as determined by gel permeation chromatography (g.p.c.) was 87000 and $\bar{M}_w/M_n$ was 2.0. The material was dissolved in boiling xylene to give a 0.1% w/v solution, which was then poured into a thin-walled glass tube held at 70°C. After 1 day, the suspension was filtered to produce a mat. After drying, the mat was pressed to remove voids: this produced a mat of thickness 60 μm, with the usual preferred orientation of lamellar normals parallel to the mat normal. Strips of width 1–2 mm were used for scattering measurements. All samples had an initial long spacing (as measured by SAXS) of 105 Å.

Annealing conditions

Two arrangements were used for heating samples:

Low heating rate. A Mettler microscope hot stage, modified with a slit cut into the heating plates, was used. The sample strip was held with mat normal perpendicular

to the X-ray beam using two aluminium plates, suitably shaped so that no aluminium was in the beam. Temperature could be controlled to within ± 0.2°C and a heating rate of 10°C min^{-1} was used. This group of samples is labelled L (low heating rate) followed by the annealing temperature (in °C).

High heating rate. A hot air blower was constructed. Compressed air was passed through a heating coil, and out through a nozzle. The direction of the nozzle was controlled by a rotary solenoid. In one position, the stream of hot air was directed onto a dummy sample in which a thermocouple was embedded. In the other position, the sample was heated directly. The air blower unit was attached to a stretching frame, the jaws of which could be closed and moved to hold and accurately position the sample with respect to the heater nozzle. The temperature of the dummy sample was used to estimate the ultimate sample temperature. Trials using thermocouples embedded in polyethylene samples indicated a time of ~ 10 s to heat a sample from room temperature to 110°C, corresponding to an average heating rate of ~ 500°C min^{-1}. With a small diameter (1 cm) nozzle, temperature gradients in the sample region are significant with a maximum of ~ 5°C min^{-1} in a direction perpendicular to both the air flow and to the centre line between the jaws. Accurate positioning of both the sample and the dummy are therefore important, and the ultimate sample temperature, although stable to within ± 1.5°C, is subject to somewhat larger uncertainties. In the discussion of results to follow, little reliance is placed on the absolute values of T_a. This group of samples is labelled H (high heating rate) followed by the annealing temperature (in °C).

MEASUREMENTS

X-ray

The SRS was used, most measurements being made on station 7.3, but with some results obtained on station 8.2. Monochromatic X-rays with wavelength 1.608 Å were used, giving a beam cross-section of about 0.4×2 mm at the sample position, with the sample strip mounted horizontally and edge-on to the X-ray beam. The sample–detector distance was 2.2 m for most measurements and a linear position-sensitive detector was used to record the scattered intensity in a vertical direction. It was found that adequate statistics were obtainable for data collection times of about 0.5 s. Longer counting times were used when changes in diffracted intensity were slow or where the intensity was very low, to make best use of time-resolved operation.

Data were corrected for two effects. First, the variation in response across the detector was compensated by calibration of the detector with a radioactive source. Second, the photon flux varies during the course of an annealing run, with a lifetime of several hours. Typical operating conditions for the SRS were 2 GeV and 200 mA. An ion chamber was used to monitor the flux of photons after the sample, and this count rate provided the necessary factor with which to correct the observed count rates.

The crystallite orientation before and after annealing was also monitored, using photographic film. The films were then scanned using an Optronics P1000 microdensitometer with a raster size of 100 μm. The GENS program (Daresbury Laboratory) was used to locate the centre of each diffraction pattern and to obtain both an averaged radial distribution and an azimuthal distribution from a 1 mm half-width annulus.

Electron microscopy

The Kanig technique was used to prepare samples suitable for electron microscopy from both unannealed and annealed mats[12]. Samples were held in chlorosulphonic acid for 43 h at 32°C. After removal, washing and drying, transverse sections were cut out using an LKB ultramicrotome. (By 'transverse' sections, we mean those where the cutting direction was parallel to the direction of lamellar normals in the original mat so that the lamellae are seen largely edge on.) Further staining made no difference to the appearance, so the samples were usually viewed unstained using a Philips 301 transmission electron microscope operating at 80 kV.

RESULTS

X-ray

Figures 1–4 show X-ray data for samples annealed at different temperatures (T_a) and with different heating rates to T_a. The variation in chosen data collection times over which scattering data were summed arises from two factors: a longer time interval was chosen (i) where the scattered intensity was particularly low and (ii) where

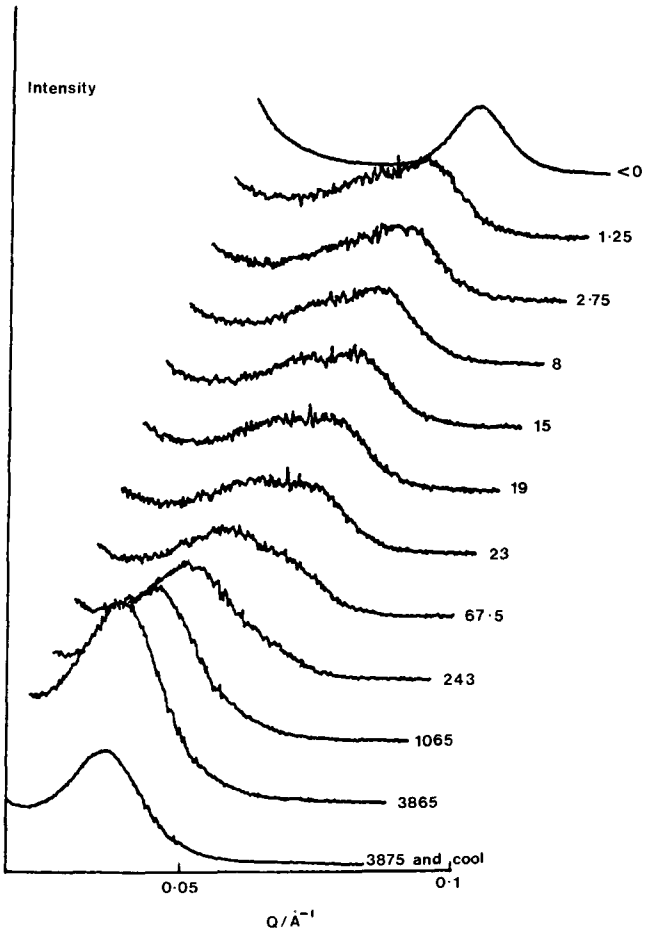

Figure 1 SAXS data for sample L122, obtained during annealing. Data acquisition times vary from 2.5 s at the start to 20 s at the end

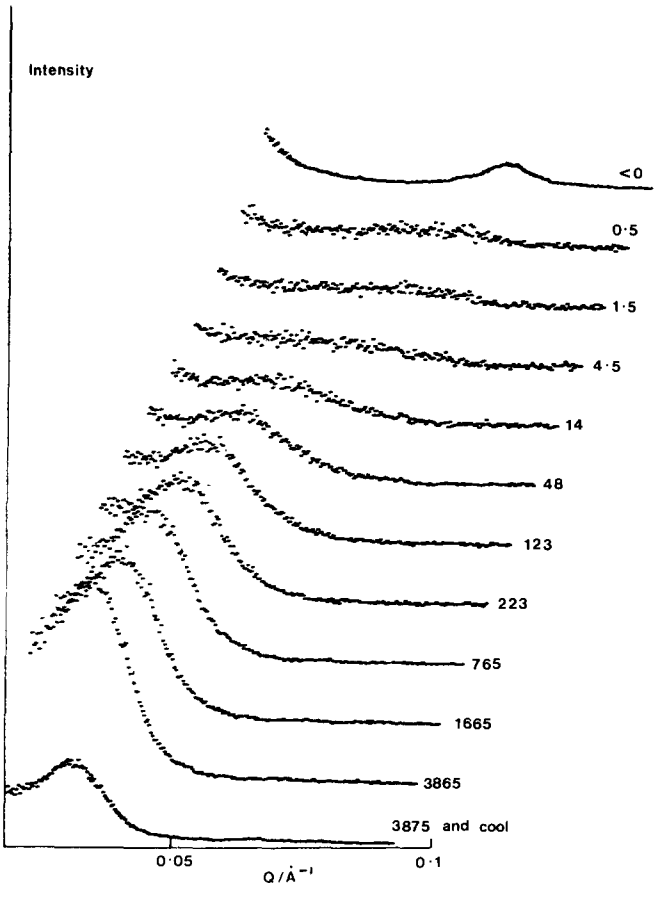

Figure 2 SAXS data for sample L126 during annealing. Data acquisition times from 1 to 20 s

the scattering was changing very slowly with time (which was the case for longest annealing times).

Several features are evident from these results. First, the initial decrease in intensity of the small-angle peak is more evident under certain conditions. For a low heating rate at $T_a = 122°C$ (*Figure 1*), the decrease in intensity is relatively minor. When T_a is raised to 126°C (*Figure 2*), the intensity rapidly decreases, with an increase in intensity becoming evident after 14 s annealing time. By contrast, the use of a high heating rate to reach T_a produces a rapid decrease in intensity (*Figures 3* and *4*) at all T_a. Enhanced intensity at the new peak position is only evident after hundreds of seconds of annealing for this annealing method.

The change in long spacing (l_x) with annealing time for low annealing temperatures is plotted after subtraction of an estimated background baseline from data such as those shown in *Figures 1–4*. The position of the peak was then determined without any intensity correction. *Figure 5* shows the familiar three-stage evolution of l_x during the course of annealing: first stage, an initial plateau region where the spacing increases only slightly with time; second stage, an abrupt increase in l_x; and third stage, a slow variation of l_x with time. This last stage includes the established linear variation of l_x with the logarithm of annealing time. However, it can be seen from *Figure 5* (sample H117) that this type of behaviour does not occur throughout the third stage, and corresponds only to annealing times greater than ~1000 s. It will be noted that the (nominal) values of T_a for the data shown in *Figure 5* are not identical. Rather,

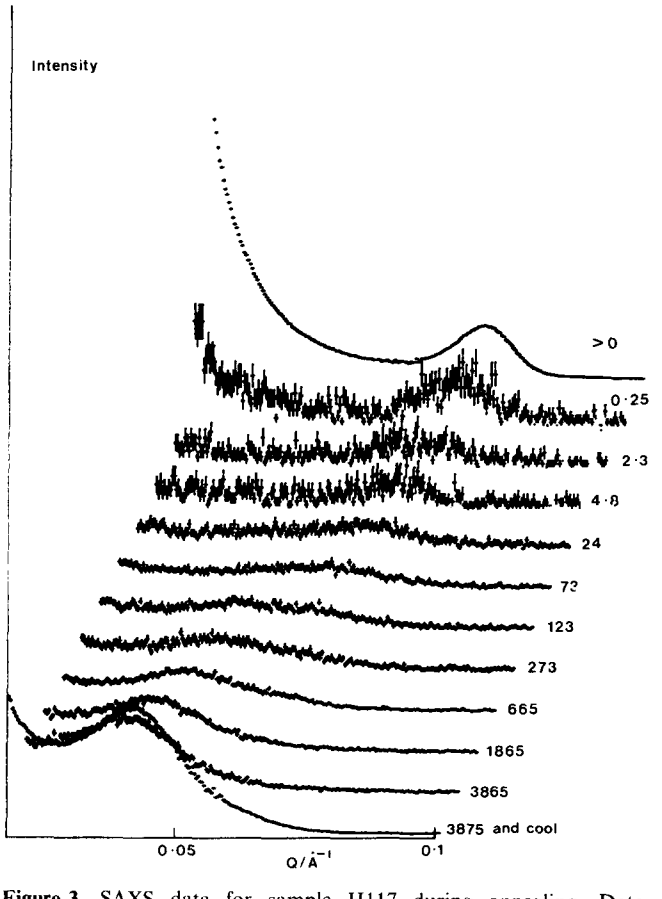

Figure 3 SAXS data for sample H117 during annealing. Data acquisition times from 0.5 to 20 s

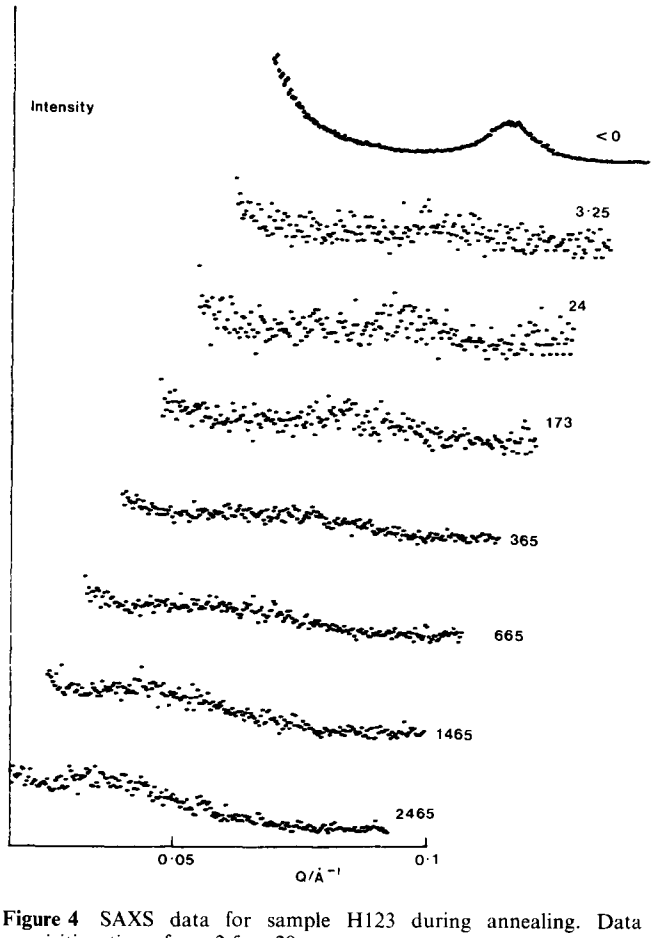

Figure 4 SAXS data for sample H123 during annealing. Data acquisition times from 2.5 to 20 s

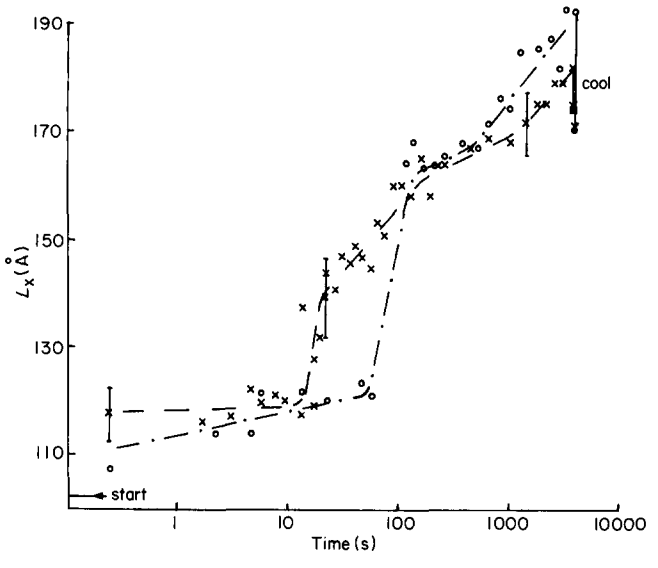

Figure 5 Variation of X-ray long spacing with annealing time for low annealing temperatures. ○, Sample H117; ×, sample L122. Lines drawn through the data are for guidance only

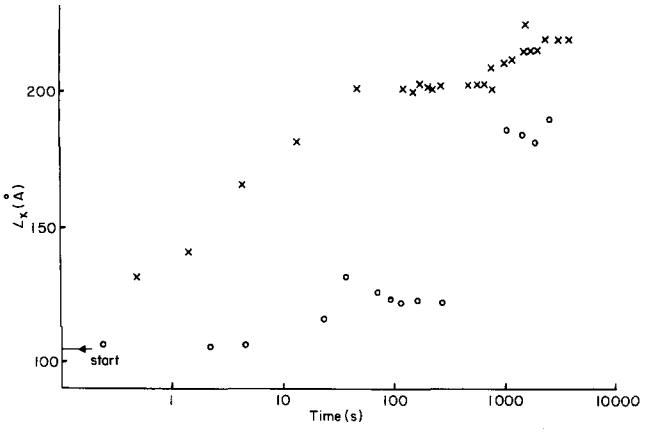

Figure 6 Variation of X-ray long spacing with annealing time for high annealing temperatures. ○, Sample H123; ×, sample L126

two annealing runs have been chosen with similar final values of l_x. Nevertheless, the route by which each sample reaches a final long spacing of ~170 Å (after similar annealing times and cooling), is clearly different in the two cases; the second phase of thickening, with its abrupt increase in spacing occurs at a longer time interval for the higher heating rate.

Note also that on final cooling, l_x decreases significantly. Electron microscopy (see next section) shows no sign of crystallites which have formed on cooling the samples, so we must conclude that the change in l_x results from a change in the stacking periodicity of the same crystals.

Data for higher annealing temperatures are shown in *Figure 6*. For the sample with the higher heating rate, the peak position is not well defined until a late stage of annealing (see *Figure 4*). Sample L126 (*Figures 2* and *6*) shows a more gradual shift in peak position, although the peak width progressively decreases.

The variation of scattered intensity is another important feature of annealing behaviour. In *Figure 7* the integrated intensity under the small-angle peak is shown as a function of annealing time for samples H117 and L122. A clear minimum appears in each plot, the position corresponding quite closely to the start of the logarithmic time dependence of lamellar thickening. The subsequent increase in intensity with annealing time is always more rapid for samples heated at lower rates.

In the absence of simultaneous WAXS and SAXS measurements, it is impossible to draw definite conclusions on the presence or absence of melting during any of these annealing experiments. A reduction in small-angle scattering intensity may arise either from a change in crystallinity or from a change in the densities of crystalline and/or amorphous phases (see equation (2)). Alternatively, the simple two-phase model discussed earlier may either be or become inadequate as a description of the annealing system. Nevertheless, it is clear that at low heating rates and annealing temperatures (*Figure 1*) there is no drastic loss in small-angle scattering intensity at any stage of annealing. We can therefore conclude that complete melting does not occur under these conditions. On the other hand, all other annealing conditions (namely slow heating rate to high T_a and high heating rate to any T_a) give rise to a dramatic loss of intensity. The presence of a minimum in the scattered intensity as a function of annealing time is almost certainly not a result of an error in determining the annealing time. Such an error might arise from underestimating the sample equilibration time. However, reference to *Figures 3* and *4* shows that it may take hundreds of seconds for the intensity to reach a minimum, a time which exceeds any estimate of the error in determining the sample equilibration time.

After cooling the annealed samples, SAXS patterns were obtained as described earlier. Typical results are shown in *Figure 8*. Azimuthal intensity scans were obtained from the densitometered films, and the result for an unannealed sample is shown in *Figure 9*. Results for both heating rates and a range of annealing temperatures are listed in *Table 1*. For the measurements at a low heating rate, the width of the small-angle peak increases slightly on annealing, but shows negligible variation with T_a. The decrease in azimuthal peak width on raising T_a from 124°C to 126°C is small and comparable with experimental errors, but leaves open the possibility of enhanced orientation at 126°C. At the

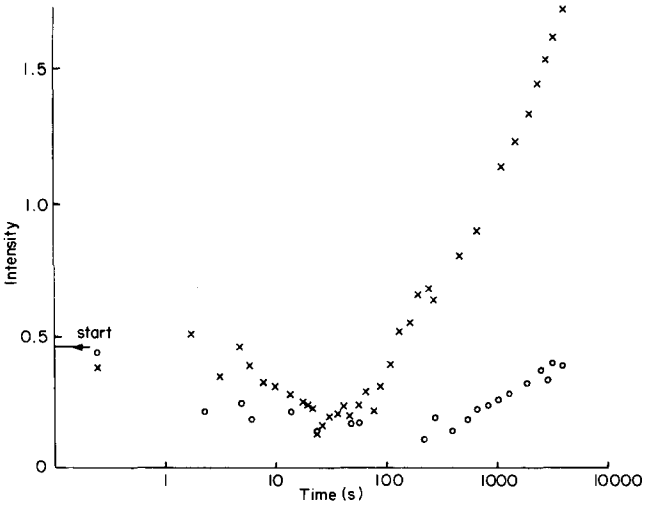

Figure 7 Variation of integrated intensity of small-angle peak with annealing time. ○, Sample H117; ×, sample L122

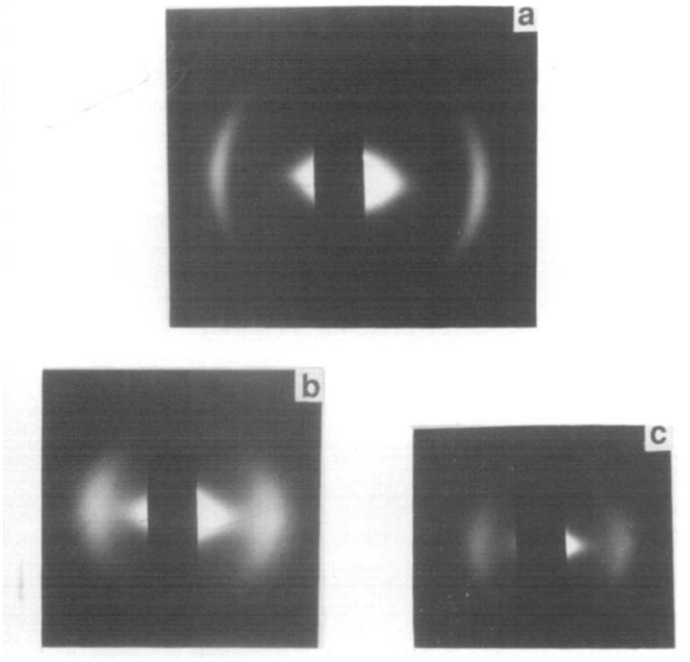

Figure 8 SAXS patterns from (a) unannealed sample; (b) H125; (c) L126; (b) and (c) are after cooling the samples

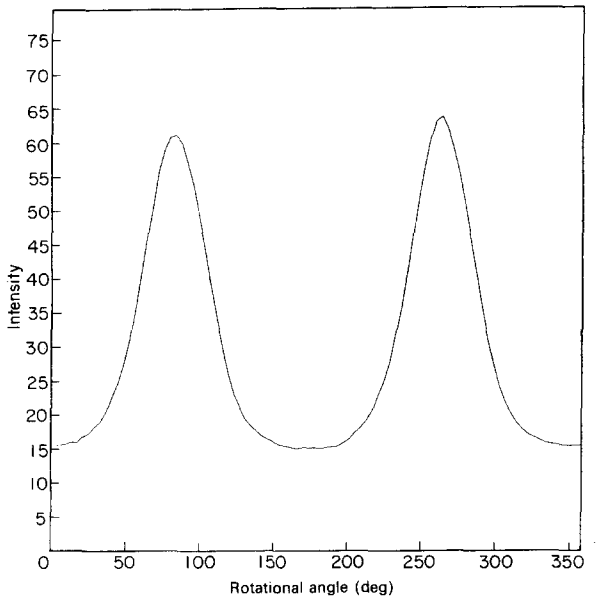

Figure 9 An azimuthal intensity scan from the data in *Figure 8a*. The radial position of the annulus taken corresponds to the maximum intensity region of the small-angle peak

higher heating rate, the disorientation of crystallites, on the basis of X-ray results, appears to be a continuous process with increasing T_a.

We conclude that the X-ray data are indicative of different annealing processes occurring at the different heating rates employed here. Evidence for this is to be found both from data obtained during annealing and from measurements after cooling. The data are consistent with the occurrence of crystal melting under conditions other than low heating rate and low T_a. For these latter conditions large scale melting does not occur.

Electron microscopy

Micrographs of unannealed and annealed samples are shown in *Figures 10–15*. The unannealed sample (*Figure 10*) shows lamellae which are continuous over a considerable distance (several micrometres) and have uniformity in both thickness and orientation. On annealing with a low heating rate (*Figures 11* and *13*), the disordering is evident. *Figure 12* again indicates disorientation, in this case for sample H117, but sample H125 (*Figure 14*) and all samples rapidly annealed to high T_a show an improvement in lamellar orientation over sample H117. This result apparently conflicts with measurements of the azimuthal width of the small-angle X-ray peak, in that the X-ray results point towards significantly more disorder in crystallite stacking at the higher T_a values. We are led to conclude that this difference is related to the different distance scales over which the measurements are made. The results may be reconciled if the H125 sample is considered to be formed of domains, within which the lamellae are well oriented, but with adjacent domains showing little correlation in direction of lamellar orientation. The size of domains would need to be large compared with the dimensions identified in micrographs. A possible mechanism for providing such domains would be recrystallization of the polymer from the melt, with a 'seed' from the original structure providing a template for (more highly oriented) deposition of lamellae within a domain.

Figure 15 shows a region in sample H125 where an

Table 1 Variation in azimuthal peak width from SAXS data

Heating rate	Annealing temperature (°C)	Azimuthal width of small angle reflection (degrees) (full width at half height ± 1°)
Low	70 (unannealed)	49
	118	54
	122	56
	124	56
	126	54
High	70 (unannealed)	49
	115	55
	117	55
	120	59
	125	63

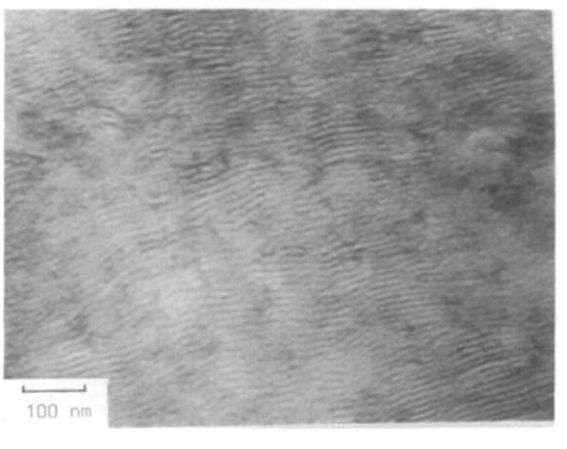

Figure 10 Transmission electron micrograph of an unannealed sample

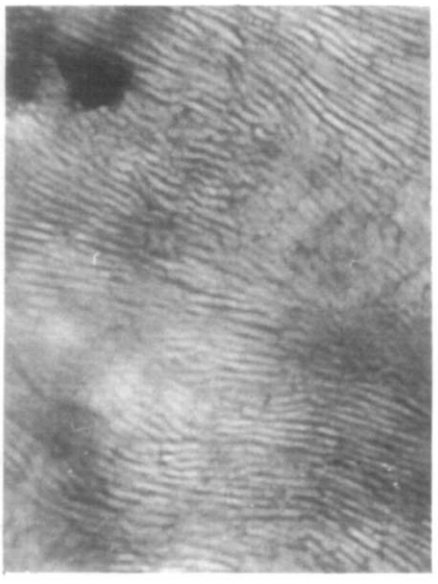

Figure 11 Transmission electron micrograph of sample L122. Scale as in *Figure 10*

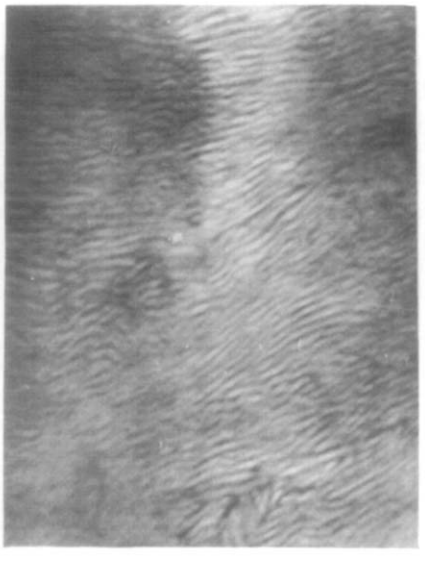

Figure 12 Transmission electron micrograph of sample H117. Scale as in *Figure 10*

abrupt change in the inclination of lamellae occurs. This is consistent with the concept of a domain boundary in such samples. Similar features were also observed for sample H123, indicating a transition to this type of behaviour occurring within the interval between 120 and 123°C.

Table 2 lists further information obtained from electron microscopy. Note that the spacings obtained from the chlorosulphonic acid fixation technique are slightly lower than those obtained from SAXS, although almost within the experimental errors. Voigt-Martin and co-workers have made extensive studies of chlorosulphonated polyethylene[13–16] and give a number of reasons why the spacings obtained may differ slightly from those given by other techniques. In our experience, the values obtained from chlorosulphonation are usually smaller than those obtained from other methods[17].

The last two columns in *Table 2* relate to the distribution of lamellar thicknesses within one sample. For the high and low heating rate pairs of samples considered, both the number of lamellae within a fixed distance in the direction of lamellar normals and its standard deviation are remarkably similar, indicating no significant difference in the population of crystal thicknesses in the two pairs of samples.

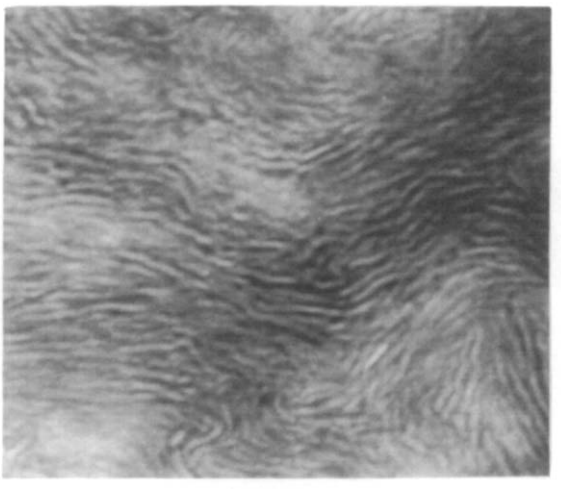

Figure 13 Transmission electron micrograph of sample L126. Scale as in *Figure 10*

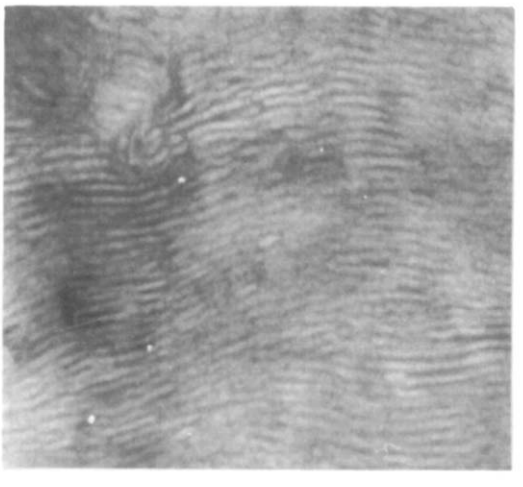

Figure 14 Transmission electron micrograph of sample H125. Scale as in *Figure 10*

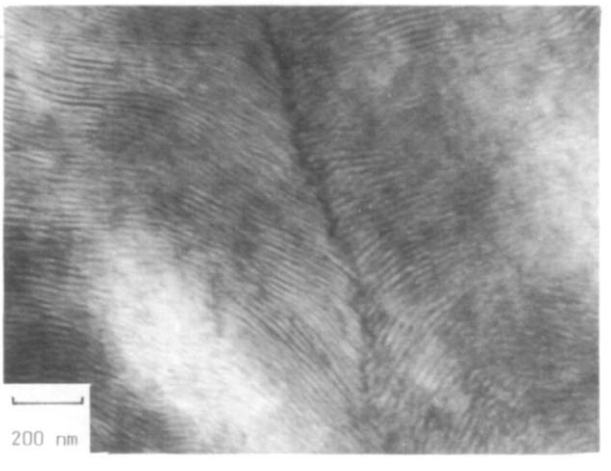

Figure 15 Transmission electron micrograph of sample H125, showing possible domain boundary

Table 2 Comparison of X-ray and electron microscopic data for annealed samples

Sample	Final X-ray long spacing (Å)	Lamellar spacing from electron micrographs (Å)	Ratio of X-ray/electron microscope spacings	Average number of lamellae within a fixed distance	Standard deviation of the average number
Unannealed	105	105	1.00	9.33	0.69
H115	145[a]	120	1.21	8.20	1.19
L118	144[a]	120	1.20	8.09	0.93
H117	162[a]	143	1.13	6.88	0.74
L122	171	144	1.19	6.84	0.62
H123	181[a]	158	1.15	6.20	0.72
L124	180	155	1.16	6.33	0.73
H125	202	186	1.09	5.29	0.72
L126	190[a]	190	1.00	5.17	0.70

[a]After cooling

The electron micrographs provide little or no evidence of lamellae which have doubled in thickness, a feature which has been discussed earlier in the context of polyethylene[18,19].

CONCLUSIONS

The X-ray measurements reported here confirm that the thickening of polyethylene single crystals during annealing generally occurs by a three-stage process. Significant differences occur when T_a is reached at different heating rates. In general, the higher heating rate leads to a more rapid and a greater loss of intensity in the small-angle peak. At lower heating rates, this reduction is less pronounced, consistent with the conclusions from previous work which suggested a localized solid state reorganization for $T_a < 123°C$[6,7]. The subsequent growth in intensity at the position of the peak due to thickened crystals is more rapid for lower heating rates.

Electron microscopy has shown that heating rate makes little difference to the distribution of lamellar thicknesses following annealing. The regularity of lamellar stacking is reduced as T_a increases, with the exception of results obtained at the highest T_a ($T_a > 120°C$) with the high heating rate.Here, an apparent conflict between X-ray diffraction data and electron microscopy can be resolved if the sample consists of well-oriented domains of lamellae, with little correlation in the orientation within different domains. Electron micrographs from samples annealed at high heating rate and $T_a > 120°C$ are consistent with this view. This domain structure, in combination with the observed initial dramatic loss of X-ray intensity at the high heating rate, is consistent with the samples undergoing melting and subsequent recrystallization around seed crystals. There is also the possibility that melting occurs to some extent at the low heating rate for the higher values of T_a studied, from the evidence of a large loss of X-ray intensity at an early stage. This conclusion is consistent with results obtained from mixed crystal infra-red spectroscopy and neutron scattering, which both indicate that the mechanism of lamellar thickening changes at $T_a \simeq 123°C$ (refs 6 and 7).

ACKNOWLEDGEMENTS

We are grateful to Professor A. Keller for his enthusiastic support, to Richard Exley for building the hot air blower /X-ray camera and to Anna Halter for assistance in sample preparation. We also thank Dr C. Nave and Dr G. Locke-Scobey (SERC Daresbury Laboratory, UK) for their assistance with X-ray measurements and densitometry.

REFERENCES

1 Fischer, E. W. and Schmidt, G. F. *Angew. Chem.* 1962, **74**, 551
2 Fischer, E. W. *Koll. Z.Z. Polym.* 1969, **231**, 458
3 Grubb, D. T., Liu, J. H., Caffrey, M. and Bilderbeck, D. H. *J. Polym. Sci., Polym. Phys. Edn* 1984, **22**, 367
4 Kawaguchi, A., Ichida, T., Murakami, S. and Katayama, K. *Colloid Polym. Sci.* 1984, **262**, 597
5 Wunderlich, B. *J. Polym. Sci. C* 1973, **43**, 29
6 Sadler, D. M. and Spells, S. J. *Macromolecules* 1989, **22**, 3941
7 Spells, S. J. and Sadler, D. M. *Macromolecules* 1989, **22**, 3948
8 Grubb, D. T. and Liu, J. H. *J. Appl. Phys.* 1985, **58**, 2822
9 Ichido, T., Tsuji, M., Murakami, S., Kawaguchi, A. and Katayama, K. *Colloid Polym. Sci.* 1985, **263**, 293
10 Schouterden, P., Vandermarliere, M., Riekel, C., Koch, M. H. J., Groeninckx, G. and Reynaers, M. *Macromolecules* 1989, **22**, 237
11 Swann, P. R. *J. Polym. Sci.* 1960, **42**, 525
12 Kanig, G. *Prog. Colloid Polym. Sci.* 1975, **57**, 176
13 Strobl, G. R., Schneider, M. J. and Voigt-Martin, I. G. *J. Polym. Sci.* 1980, **18**, 1361
14 Voigt-Martin, I. G., Fischer, E. W., Hagedorn, W., Hendra, P. and Mehler, K. Abstracts of 26th International IUPAC Symposium, Mainz, 1979, p. 1250
15 Voigt-Martin, I. G. and Mandelkern, L. *J. Polym. Sci.* 1981, **19**, 1769
16 Voigt-Martin, I. G. *Polym. Prepr.* 1989, **30**, 293
17 Bashir, Z., Hill, M. J. and Keller, A. *J. Mater. Sci. Lett.* 1986, **5**, 876
18 Nagatoshi, F. and Takayanagi, M. *Reports Prog. Polym. Phys. Jpn* 1964, **7**, 77
19 Fischer, E. W. *Pure Appl. Chem.* 1972, **31**, 113